

https://dspace.org/

# The generation of human induced pluripotent stem cell lines from individuals of Black African ancestry in South Africa

**J Naidoo; T Hurrell; Janine Scholefield**

https://hdl.handle.net/10539/44176
WOS

Downloaded from a DSpace repository. https://dspace.org/

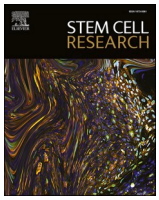
Stem Cell Research 81 (2024) 103534



Contents lists available at ScienceDirect

Stem Cell Research

journal homepage: www.elsevier.com/locate/scr



Lab Resource: Multiple Cell Lines



# The generation of human induced pluripotent stem cell lines from individuals of Black African ancestry in South Africa

Jerolen Naidoo [a,b,1], Tracey Hurrell [a,1], Janine Scholefield [a,b,c,*]

[a] Bioengineering and Integrated Genomics Group, Future Production: Chemicals Cluster, Council for Scientific and Industrial Research, PO Box 395, Pretoria 0001, South Africa
[b] Department of Human Biology, Faculty of Health Sciences, University of Cape Town, Private Bag X3, Rondebosch 7701, South Africa
[c] Division of Human Genetics, Faculty of Health Sciences, University of the Witwatersrand, PO Box 1038, Johannesburg 2000, South Africa

ARTICLE INFO

*Keywords:*
hiPSC
African ancestry
African representation
Hepatocyte-like cells
Cortical neurons

ABSTRACT

The lack of equitable representation of African diversity in scientific resources, such as genome-wide association studies and human induced pluripotent stem cell (hiPSC) repositories, has perpetuated inequalities in the advancement of health research. HiPSCs could be transformative in regenerative and precision medicine, therefore, the generation of diverse lines is critical in the establishment of African-relevant preclinical cellular models. HiPSC lines were derived from two healthy donors of Black African ancestry using Sendai virus reprogramming of dermal fibroblasts, and characterised to confirm stemness markers, trilineage differentiation, and genetic integrity. These hiPSCs represent a valuable resource for modelling African relevant disease biology.

## Resource Table

| | |
|---|---|
| Unique stem cell lines identifier | CSIRi001-B<br>CSIRi001-A<br>CSIRi002-A<br>CSIRi002-B |
| Alternative names of stem cell lines | CSIR-SA-001-J3 (CSIRi001-B)<br>CSIR-SA-001-J4 (CSIRi001-A)<br>CSIR-SA-001-L2 (CSIRi002-A)<br>CSIR-SA-001-L10 (CSIRi002-B) |
| Institution | Council for Scientific and Industrial Research (CSIR), South Africa |
| Contact information of distributor | jscholefield@csir.co.za |
| Type of cell lines | iPSCs |
| Origin | Human |
| Cell Source | iPSCs were derived from human dermal fibroblasts from donors of African genetic ancestry |
| Clonality | Clonal |
| Method of reprogramming | Sendai virus (OKSM) |
| Multiline rationale | N/A |
| Gene modification | N/A |
| Type of modification | N/A |

(*continued on next column*)

**Resource Table** (*continued*)

| | |
|---|---|
| Unique stem cell lines identifier | CSIRi001-B<br>CSIRi001-A<br>CSIRi002-A<br>CSIRi002-B |
| Associated disease | N/A |
| Gene/locus | N/A |
| Method of modification | N/A |
| Name of transgene or resistance | N/A |
| Inducible/constitutive system | N/A |
| Date archived/stock date | N/A |
| Cell line repository/bank | Registered in the Human Pluripotent Stem Cell Registry (https://hpscreg.eu) |
| Ethical approval | Approval granted by CSIR REC (Ref: 77_2013, approved 21/01/2019), in line with approval from the University of the Witwatersrand (M190221) approved 29/04/2019. |

* Corresponding author at: Bioengineering and Integrated Genomics Group, Future Production: Chemicals Cluster, Council for Scientific and Industrial Research, PO Box 395, Pretoria 0001, South Africa.
*E-mail address:* JScholefield@csir.co.za (J. Scholefield).
[1] Equal contribution

https://doi.org/10.1016/j.scr.2024.103534
Received 25 May 2024; Received in revised form 2 August 2024; Accepted 9 August 2024
Available online 10 August 2024
1873-5061/© 2024 The Authors. Published by Elsevier B.V. This is an open access article under the CC BY-NC license (http://creativecommons.org/licenses/by-nc/4.0/).

## 1. Resource utility

The generation of vast numbers of hiPSC lines inclusive of African genetic diversity represents an important objective towards attaining equitable representation of African datasets in global scientific resources (Ghosh et al., 2022; Wonkam, 2021). A total of four human induced pluripotent stem cell (hiPSC) lines were generated from human dermal fibroblasts (HDFs) derived from two donors i.e. a healthy female donor of Black-=African ancestry in South Africa, who self-identified as being of Zulu ethnolinguistic origin (CSIR-SA-001-J 3/4), as well from a commercially available fibroblast line, also of Black African ancestry (CSIR-SA-001-L 2/10) but unknown ethnolinguistic origin (Table 1). These lines represent a potentially valuable resource for the development of African-relevant biomedical research tools (Naidoo et al., 2022).

## 2. Resource details

Despite harbouring population groups with the greatest genetic diversity globally (Choudhury et al., 2020), the African continent continues to be significantly underrepresented in global scientific resources like Genome-Wide Association Studies (GWAS) databases (Sirugo et al., 2019) and hiPSC repositories (Ghosh et al., 2022). HiPSC technologies hold great promise as a tool for biomedical innovation within the fields of regenerative and precision medicine (Hurrell et al., 2022; Veale et al., 2023).

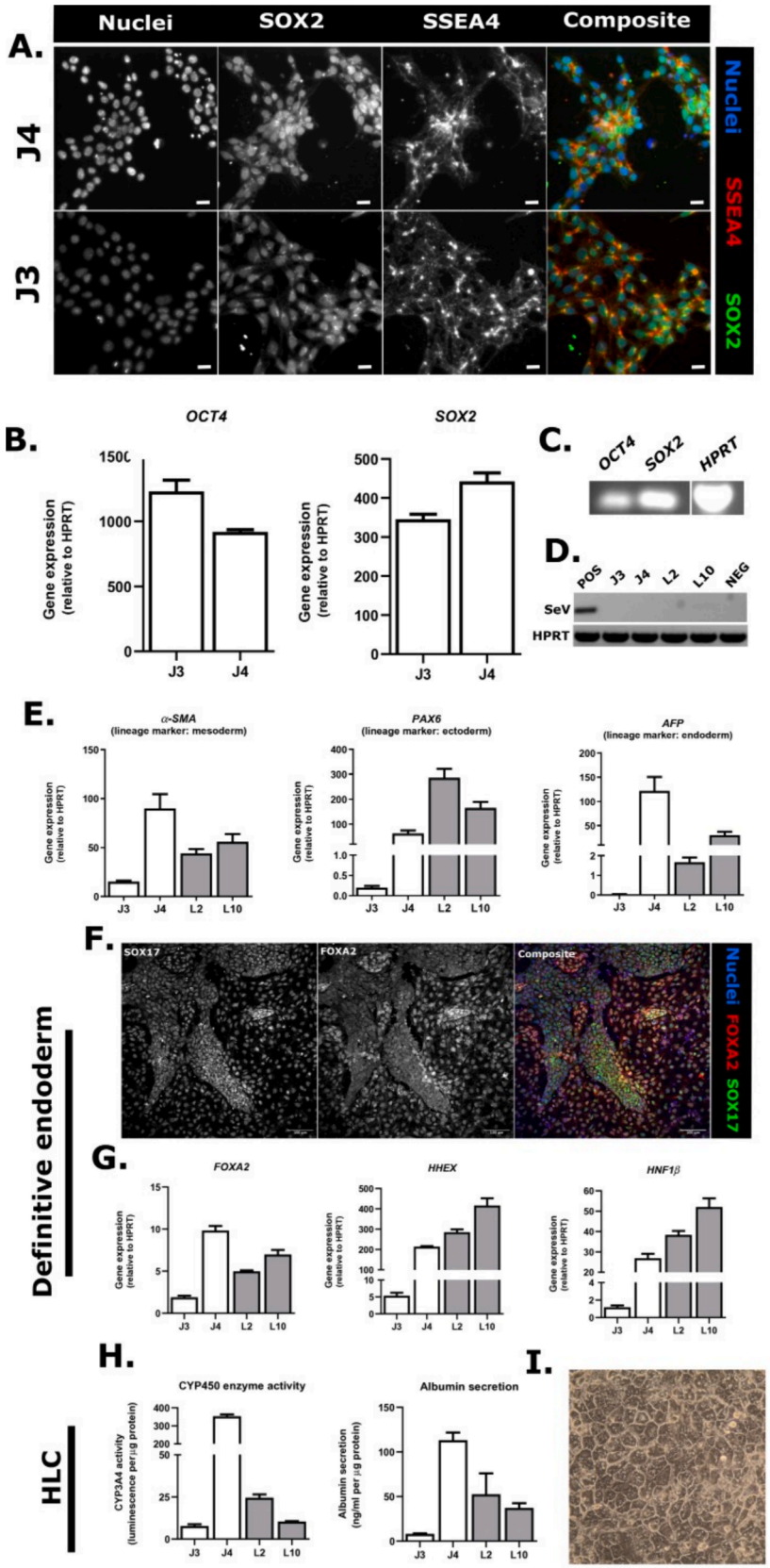
The CSIR-SA-001-J3 (J3), CSIR-SA-001-J4 (J4), CSIR-SA-001-L2 (L2), and CSIR-SA-001-L10 (L10) hiPSC lines were generated from human dermal fibroblasts (HDFs) through the expression of Yamanaka factors (OCT4, KLF4, SOX2, and c-MYC) using non-integrating Sendai virus (Ban et al., 2011). The J3 and J4 lines were derived from a self-identified Black African donor of Zulu ethnolinguistic origin, while L2 and L10 lines were derived from a commercially available fibroblast cell line originating from a donor of Black African ancestry. All lines exhibited classical hiPSC morphology and passed standard characterisation for stemness markers (Table 2). The J4, L2, and L10 lines all exhibited normal karyotypes (46 XY/ XX) ten passages into feeder-free culture following copy number variation (CNV) analyses, however the J3 line exhibited chromosome 20 trisomy (47, XX, seq(20)x3). While the J3 line therefore did not meet acceptable quality control standards for a validated hiPSC line (Supplementary Fig. S1) it was still included in subsequent experimental validations as a chromosome 20 trisomy phenotypic control. The expression of stemness markers (OCT4, SSEA4, SOX2) were confirmed by immunofluorescence microscopy between passages 15 and 20, and the expression of OCT4, SOX2, and NANOG were confirmed by RT-PCR (Fig. 1A-C and Fig. S2A-D). Sendai virus (SeV) clearance in hiPSC lines was confirmed by RT-PCR with early passage lines as a positive control and RNA isolated from a HepG2 cell lines as a negative control (Fig. 1D). Lines displayed classical hiPSC morphology and colony structure as per brightfield microscopy (Fig. S3A). Trilineage (germ layer) differentiation potential was evaluated using a spontaneous differentiation strategy following embryoid body (EB) formation (Fig. 1E, Fig. S3B). The expression of specific lineage markers for endoderm (AFP), ectoderm (PAX6), and mesoderm (αSMA) were confirmed by RT-PCR for all cell lines at day 14 of spontaneous differentiation (Fig. 1F). The J3 line, however, displayed a markedly reduced capacity for germ layer differentiation when compared to the other lines. Mycoplasma screening was conducted using high resolution imaging which confirmed that all lines were free of mycoplasma contamination (Fig. S4). Short tandem repeat (STR) analysis confirmed the iPSC lines were derived from their respective parental donor fibroblast lines. The terminal differentiation capacity of specific lines was also evaluated using directed differentiation of both endoderm derived hepatocyte-like cells (HLCs, Fig. 1F) and ectoderm-derived cortical neurons (Fig. S3). For HLC differentiation, the expression of endoderm markers SOX17, FOXA2, HHEX, and HNF1ß were confirmed at day 6 of directed endoderm differentiation by either immunofluorescence microscopy or RT-PCR (Fig. 1G). Notably the J3 line again revealed reduced capacity for endoderm differentiation as compared to the J4, L2, and L10 lines across all markers assayed by RT-PCR. The functional validation of terminally differentiated HLCs revealed robust CYP450 (CYP3A4) enzymatic activity and albumin protein secretion across the J4, L2, and L10 lines (Fig. 1H). In accordance with the trend of reduced differentiation capacity observed at the endoderm stage, the J3 line also revealed markedly reduced CYP450 enzymatic activity and albumin secretion within derived HLC populations. Brightfield microscopy revealed distinct hepatocyte-like morphology following

**Table 2**
Characterization and validation.

| Classification | Test | Result | Data |
|---|---|---|---|
| Morphology | Brightfield microscopy | Normal | Fig. S2A |
| Phenotype | Qualitative analysis −Immunocytochemistry | Staining of stemness markers – OCT4, SSEA4, SOX2 | Fig. 1A and S1 |
| | Quantitative analysis – RT-PCR | Gene expression of stemness markers – OCT4, SOX2, NANOG | Fig. 1B, C and S1 |
| Genotype | Copy number variation (CNV) | SA-CSIR-J3: 47, XX, seq(20)x3<br>SA-CSIR-J4: 46, XX<br>SA-CSIR-L2: 46, XY<br>SA-CSIR-L10: 46, XY | Fig. S4 |
| Virology and microbiology | Sendai virus | Negative by PCR | Fig. 1D |
| | Mycoplasma | Negative by high resolution fluorescent microscopy | Fig. S3 |
| Differentiation potential | Spontaneous differentiation | Embryoid body formation and gene expression of germ layer markers – αSMA, PAX6, AFP | Fig. 1F and S2B |
| | Guided differentiation – hepatocyte-like cells | Staining of endoderm markers – SOX17, FOXA2<br>Gene expression of endoderm markers – FOXA2, HHEX, HNF1β<br>Functional analysis – CYP450 enzyme activity and albumin secretion | Fig. 1F–I |
| | Guided differentiation – cortical neurons | Staining of neural precursor and cortical neuron makers – PAX6, TUBB3, and MAP2 | Fig. S5 |

**Table 1**
Summary information of hiPSC line origin.

| hiPSC line name | Abbreviation | Gender | Ethnolinguistic origin | Ancestry | Disease |
|---|---|---|---|---|---|
| CSIR-SA-001-J3 | J3 | Female | Zulu | African | None |
| CSIR-SA-001-J4 | J4 | Female | Zulu | African | None |
| CSIR-SA-001-L2 | L2 | Male | Unknown | African | Unknown |
| CSIR-SA-001-L10 | L10 | Male | Unknown | African | Unknown |




(caption on next page)

**Fig. 1.** Characterisation of hiPSC lines and hepatocyte-like cell differentiation. Positive SOX2 and SSEA4 staining in J3 and J4 lines, nuclei counterstained with Hoechst, scale bars = 20 μm (A). Confirmation of *OCT4* and *SOX2* gene expression by RT-PCR, expression relative to HPRT (B). Confirmation of RT-PCR amplicons by gel electrophoresis (C). Confirmation of Sendai virus (SeV) clearance by PCR, RNA from early passage stocks were used as a positive control (POS), RNA from HepG2 cell line used as a negative control (NEG). All lines confirmed to be free of SeV by gel electrophoresis (D). Characterisation of trilineage differentiation potential using spontaneous differentiation and RT-PCR to confirm the expression of specific marker genes for each germ layer (*α-SMA*: mesoderm, *PAX6*: ectoderm and *AFP*: endoderm). Gene expression relative to *HPRT* (E). Positive staining of definitive endoderm markers, FOXA2 and SOX17, with in nuclei counterstained with Hoechst in J4 line, scale bars = 20 μm representing (F). Confirmation of *FOXA2, HHEX,* and *HNF1β* gene expression by RT-PCR, expression relative to *HPRT* (G). Confirmation of HLC function using CYP450 enzyme activity and albumin secretion (H). Brightfield microscopy image of HLC morphology (I).

differentiation to HLCs (Fig. 1I). For neuronal differentiation, the expression of OCT4 and absence of neural specification marker, PAX6, was observed at day 2 following differentiation to neural precursor cells (Fig. S5), while the absence of OCT4 and expression of PAX6 was observed by day 7 using immunofluorescence microscopy (Fig. S5). The expression of intermediate (TUBB3) and mature (MAP2) neuronal markers were observed at day 26 of neuronal differentiation along with classical neuronal morphology (Fig. S5).

## 3. Materials and methods

### 3.1. Cell culture and reprogramming

Human dermal fibroblasts (HDF) were obtained from skin puncture biopsies from a consenting adult donor (CSIR-J) and purchased from Lonza (CSIR-L; NHDF #CC-2511, Lot 23801). Cells were cultured in DMEM-F12 for two days before reprogramming using the CytoTune-iPS 2.0 Sendai reprogramming kit as per the manufacturer's instructions (Thermo Fisher Scientific). Established hiPSC lines were transitioned to and maintained under feeder-free conditions in Essential 8 media (E8; Gibco) on Geltrex-coated (Gibco) tissue culture vessels. Cells were passaged every 3–4 days using TrypLE, and seeded at 30 000 cells/cm$^2$ in E8 media supplemented with Y-27632 (10 μM; Tocris). Fresh E8 media, without Y-27632, was added daily. All cells were cultured in a 37 °C incubator with 5 % $CO_2$.

### 3.2. Sendai clearance

The inactivation and clearance of Sendai virus (SeV) from hiPSCs was evaluated using RT-PCR. Total RNA was isolated using Direct-zol RNA isolation kit (Zymo Research) and 200 ng total RNA was reverse transcribed using a SuperScript IV first-strand synthesis system (Invitrogen). PCRs were prepared using DreamTaq Green PCR Master Mix and performed on a T100 thermal cycler (Bio-Rad). Pooled RNA isolated from early passage hiPSC lines was used as a positive control for SeV detection and RNA isolated from a HepG2 cell line was used a negative control. PCR products were analysed using agarose gel electrophoresis and ethidium bromide staining.

### 3.3. Mycoplasma screening

Mycoplasma screening of hiPSCs was conducted using fluorescent microscopy. Briefly, hiPSC lines were seeded onto glass coverslips at a density of 30 000 cells/cm$^2$ in E8 media supplemented with Y-27632 (10 μM). Cells were transitioned to E8 media only after 24 h, following and additional 24 h of culture, cells were fixed in 3.7 % formaldehyde solution (Sigma-Aldrich) in 1x PBS for 10 min at room temperature. Cells were permeabilised in 70 % ethanol (Sigma-Aldrich) for 4 h at room temperature and counter-stained with Hoechst (2 μM) for 20 min at room temperature. Images were acquired on a Zeiss AiryScan LSM (Zeiss GmbH) using the 100x objective and super-resolution imaging module to screen for extranuclear Hoechst-positive signal.

### 3.4. Analysis of copy number variation

Genomic DNA was isolated from hiPSCs and whole-chromosome aneuploidies, and segmental gains and losses (>10Mbp) were detected using low coverage next generation sequencing (Next Biosciences; Midrand, South Africa).

### 3.5. Short tandem repeat analysis

Short tandem repeat (STR) analysis was performed on cell pellets from each parental and daughter cell lines using 27 loci which included amelogenin (Ampath Laboratories; Centurion, South Africa).

### 3.6. Trilineage differential potential

The differentiation potential of hiPSCs was determined using a spontaneous differentiation strategy (Aqel et al., 2020). Briefly, embryoid bodies were formed by seeding 3000 cells per microwell in a MicroTissues® 3D Petri Dish® micro-mold (9 x 9 array; 12–81) in E8 media supplemented with Y-27632 (10 μM). Embryoid bodies were subsequently cultured for 4 days in KnockOut DMEM supplemented with Knockout Serum Replacement (KOSR − 20 %; Gibco), L-glutamine (1 mM; Gibco), non-essential amino acids (1 %; Gibco), and beta-mercaptoethanol (0.1 mM; Gibco). Embryoid bodies were then transferred to Geltrex-coated plates for an additional 10 days before analysis of lineage markers.

### 3.7. Hepatocyte-like cell differentiation

Differentiation of hiPSC to hepatocyte-like cells (HLCs) was conducted using a growth-factor based protocol (Raggi et al., 2022). hiPSCs were seeded (50 000 cells/cm$^2$) on Geltrex-coated plates in E8 media supplemented with Y-27632 (10 μM). Differentiation to definitive endoderm was initiated using RPMI-B27 minus insulin (Gibco) supplemented with 1 % KOSR, Activin A (100 ng/ml; Miltenyi Biotec) and CHIR99021 (3 μM; Sigma) for 2 days followed by 3 days with Activin A only. Following induction of definitive endoderm, cells were harvested for analysis, or continued through sequential phases of ventral posterior foregut, liver bud, and HLC maturation as described by Raggi et al. (2022). HLCs were differentiated to day 30 and assessed for functional outcomes by measuring CYP450 enzyme activity and albumin secretion.

### 3.8. Cortical neuron differentiation

Differentiation of hiPSC to cortical neurons was initiated using dual SMAD inhibition to derive neural precursor cells (Shi et al., 2012). hiPSCs were seeded (60 000 cells/cm$^2$) on Geltrex-coated plates in Essential 8 media supplemented with Y-27632 (10 μM). hiPSC were differentiated for 7 days in neural induction media containing 1:1 mixture of B27-containing and N2-containing media (Gibco) with LDN193189 dihydrochloride (100 nM; Tocris) and SB431542 (10 μM; Tocris). Neural precursor cells were characterized via immunocytochemistry on day 2 and day 7. Cells were further cultured in neural maintenance media (1:1 B27-containing and N2-containing media) and passaged every 3–4 days until day 20. Cells were then seeded on Geltrex-coated plates for differentiation into cortical neurons and cultured in B27-containing media with DAPT (10 μM; Tocris) before characterization via immunocytochemistry at day 26.

### 3.9. Gene expression analysis

Total RNA was isolated using Direct-zol RNA isolation kit (Zymo Research) and 200 ng total RNA was reverse transcribed using a SuperScript IV first-strand synthesis system (Invitrogen). Quantitative polymerase chain (RT-PCR) reaction was performed using SsoAdvanced Universal SYBR Green Supermix (Bio-Rad) on a CFX96 real-time PCR system (Bio-Rad). Gene expression of selected primers (Table 3) was analysed using the $2^{-\Delta\Delta}$ Ct method (Livak and Schmittgen, 2001).

### 3.10. Immunocytochemistry and imaging

HiPSCs were seeded and differentiated on either Geltrex-coated glass coverslips or Geltrex-coated 96-well imaging plates (Nunc). At each endpoint, cells were fixed in 3.7 % formaldehyde solution (Sigma-Aldrich) in 1x PBS for 10 min at room temperature. Fixed cells were permeabilised in 70 % ethanol (Sigma-Aldrich) for 4 h at room temperature and blocked in 1 % bovine serum albumin (BSA; Sigma Aldrich) in PBS-Tween solution (0.05 %) for 30 min at room temperature. Primary antibodies (Table 3) were incubated overnight at 4℃ with secondary antibody incubations at room temperature for 1 h. Cells were counter-stained with Hoechst (2 μM) for 20 min at room temperature and images were acquired on either a Zeiss Cell Discoverer 7 (Zeiss GmbH) at the African Microscopy Initiative at the University of Cape Town or on an Olympus IX83 confocal system (Olympus). Images were processed using FIJI (Schindelin et al., 2012).

### 3.11. Albumin ELISA

The Human Serum Albumin Human ELISA Kit (EHALB; Themo Fisher Scientific) was used to quantify albumin secreted from hepatocyte-like cells. Cell culture media was harvested, debris was pelleted (1000 g; 5 min), and the supernatant stored until analysis. Sample (100 μl) was loaded onto a precoated 96-well strip plate, and the protocol conducted per the manufacturer's instructions. Absorbance was measured at 450 nm on a Tecan INFINITE F500 microplate reader. For normalization, cells were harvested directly from the well using RIPA buffer (Sigma-Aldrich) containing EDTA-free protease inhibitor cocktail (Sigma Aldrich) and clarified by centrifugation (16 000 g; 10 min). Protein was quantified using the bicinchoninic acid assay, as per manufacturer's instructions, and absorbance measured at 620 nm on a Tecan INFINITE F500 microplate reader.

### 3.12. CYP3A4 analysis

CYP3A4 activity was assessed using non-lytic P450-Glo CYP3A4 (V9002, Promega) assay with minor modifications from the manufacturer's instructions. Hepatocyte-like cells, differentiated to day 30, were washed with PBS and incubated with Luciferin-IPA (3 μM) in Kreb-Henseleit buffer (Sigma) for 1 h at 37 °C. The substrate was removed, mixed with equal parts detection reagent and incubated for 10 min at room temperature. Luminescence was measured on a Tecan INFINITE F500 microplate reader and normalized to protein content per well.

## 4. Ethics

This research was conducted in accordance with the guidelines of the Declaration of Helsinki and approved by the CSIR REC (Ref: 77_2013, approved 21/01/2019), in line with REC from the University of the Witwatersrand (M190221) approved 29/04/2019.

## Funding

Funding provided by the Council of Scientific and Industrial Research (CSIR) and the National Research Foundation (NRF) Thuthuka Funding Instrument (TTK200320510301; Grant No: 129507).

**Table 3**
Reagents details.

| **Immunocytochemistry** | | | |
|---|---|---|---|
| | **Antibody** | **Dilution** | **Company / catalogue number** |
| Stemness marker | OCT4-rabbit mAb | 1/100 | Cell Signalling Technology 2890S |
| Stemness marker | SSEA4-mouse mAb | 1/100 | Cell Signalling Technology 4755S |
| Stemness marker | SOX2-rabbit mAb | 1/50 | Abcam ab67959 |
| Endoderm marker | FOXA2-rabbit mAb | 1/100 | Abcam ab48074 |
| Endoderm marker | SOX17-mouse mAb | 1/100 | Abcam ab84990 |
| Neural precursor marker | PAX6-rabbit mAb | 1/100 | Cell Signalling Technology 60433S |
| Cortical neuron marker | MAP2-rabbit mAB | 1/200 | Cell Signalling Technology 8707S |
| Cortical neuron marker | TUBB3-rabbit mAb | 1/1000 | Abcam ab78078 |
| Proliferation marker | Ki67-mouse mAb | 1/100 | Abcam ab238020 |
| MitoTracker deep red | – | 500 nM | Thermo Scientific M22426 |
| Secondary antibody | Anti-mouse 488 | 1/500 | Abcam Ab510117 |
| Secondary antibody | Anti-rabbit 647 | 1/500 | Life Technologies A21245 |
| **Primers** | | | |
| | **Target** | **Forward / reverse (5′-3′)** | |
| Sendai virus | SeV | GGATCACTAGGTGATATCGAGC / ACCAGACAAGAGTTTAAGAGATATGTAT | |
| Stemness marker | OCT4 | GACAGGGGGAGGGGAGGAGCTAGG / CTTCCCTCCAACCAGTTGCCCCAAAC | |
| Stemness marker | SOX2 | GGGAAATGGGAGGGGTGCAAAAGAGG / TTGCGTGAGTGTGGATGGGATTGGTG | |
| Stemness marker | NANOG | CATGAGTGTGGATCCAGCTTG / CCTGAATAAGCAGATCCATGG | |
| Unguided – endoderm marker | AFP | TGGGACCCGAACTTTCCA / GGCCACATCCAGGACTAGTTTC | |
| Unguided – mesoderm marker | αSMA | TATCCCCGGGACTAAGACGG / CACCATCACCCCCTGATGTC | |
| Unguided – ectoderm marker | PAX6 | CAGAGCCCCATATTCGAGCC / CAAAGACACCACCGAGCTGA | |
| Endoderm marker | FOXA2 | CATGCACTCGGCTTCCAGTA / CGTGTTCATGCCGTTCATCC | |
| Endoderm marker | HHEX | CAGCGAGAGACAGGTCAAAAC / TGGGCAAATCTTGCCTCTGAT | |
| Endoderm marker | HNF1β | CCCTTGGAGGGCTGCTAAAA / GGACTGTCTGGTTGAATTGTCG | |
| Reference gene | HPRT | GCAGCCCTGGCGTCGTGATTA / CGTGGGGTCCTTTTCACCAGCA | |

## CRediT authorship contribution statement

**Jerolen Naidoo:** Writing – original draft, Methodology, Funding acquisition, Formal analysis, Data curation, Conceptualization. **Tracey Hurrell:** Writing – review & editing, Writing – original draft, Methodology, Funding acquisition, Formal analysis, Data curation, Conceptualization. **Janine Scholefield:** Writing – review & editing, Supervision, Project administration, Methodology.

## Declaration of competing interest

The authors declare that they have no known competing financial interests or personal relationships that could have appeared to influence the work reported in this paper.

## Acknowledgements

The authors would like to thank Wirsam Scientific for kindly

granting us access to the Olympus iX83 confocal microscope system for stemness and HLC characterisation. The microscope systems used for stemness and neuronal characterisation were accessed through the African Microscopy Initiative (AMI) visiting researcher programme at the University of Cape Town (South Africa). In addition, the authors would like to thank Brian Kariithi for consenting the CSIR-SA-J donor.

## Appendix A. Supplementary data

Supplementary data to this article can be found online at https://doi.org/10.1016/j.scr.2024.103534.

## References

Aqel, Y.W.A., Ali, G., Elsayed, A.K., Al-Khawaga, S., Hussain, K., Abdelalim, E.M., 2020. Generation of two human iPSC lines from patients with maturity-onset diabetes of the young type 2 (MODY2) and permanent neonatal diabetes due to mutations in the *GCK* gene. Stem Cell Research 48, 101991. https://doi.org/10.1016/j.scr.2020.101991.

Ban, H., Nishishita, N., Fusaki, N., Tabata, T., Saeki, K., Shikamura, M., Takada, N., Inoue, M., Hasegawa, M., Kawamata, S., Nishikawa, S.-I., 2011. Efficient generation of transgene-free human induced pluripotent stem cells (iPSCs) by temperature-sensitive Sendai virus vectors. Proceedings of the National Academy of Sciences 108, 14234–14239. https://doi.org/10.1073/pnas.1103509108.

Choudhury, A., Aron, S., Botigué, L.R., Sengupta, D., Botha, G., Bensellak, T., Wells, G., Kumuthini, J., Shriner, D., Fakim, Y.J., Ghoorah, A.W., Dareng, E., Odia, T., Falola, O., Adebiyi, E., Hazelhurst, S., Mazandu, G., Nyangiri, O.A., Mbiyavanga, M., Benkahla, A., Kassim, S.K., Mulder, N., Adebamowo, S.N., Chimusa, E.R., Muzny, D., Metcalf, G., Gibbs, R.A., Rotimi, C., Ramsay, M., Adeyemo, A.A., Lombard, Z., Hanchard, N.A., 2020. High-depth African genomes inform human migration and health. Nature 586, 741–748. https://doi.org/10.1038/s41586-020-2859-7.

Ghosh, S., Nehme, R., Barrett, L.E., 2022. Greater genetic diversity is needed in human pluripotent stem cell models. Nat Commun 13, 7301. https://doi.org/10.1038/s41467-022-34940-z.

Hurrell, T., Naidoo, J., Scholefield, J., 2022. Hepatic Models in Precision Medicine: An African Perspective on Pharmacovigilance. Front Genet 13, 864725. https://doi.org/10.3389/fgene.2022.864725.

Livak, K.J., Schmittgen, T.D., 2001. Analysis of Relative Gene Expression Data Using Real-Time Quantitative PCR and the $2-\Delta\Delta CT$ Method. Methods 25, 402–408. https://doi.org/10.1006/meth.2001.1262.

Naidoo, J., Hurrell, T., Scholefield, J., 2022. IPSC-derived models in Africa: An HIV perspective. Biochimie, Regeneration in Health and Disease 196, 153–160. https://doi.org/10.1016/j.biochi.2022.01.013.

Raggi, C., M'Callum, M.-A., Pham, Q.T., Gaub, P., Selleri, S., Baratang, N.V., Mangahas, C.L., Cagnone, G., Reversade, B., Joyal, J.-S., Paganelli, M., 2022. Leveraging interacting signaling pathways to robustly improve the quality and yield of human pluripotent stem cell-derived hepatoblasts and hepatocytes. Stem Cell Reports 17, 584–598. https://doi.org/10.1016/j.stemcr.2022.01.003.

Schindelin, J., Arganda-Carreras, I., Frise, E., Kaynig, V., Longair, M., Pietzsch, T., Preibisch, S., Rueden, C., Saalfeld, S., Schmid, B., Tinevez, J.-Y., White, D.J., Hartenstein, V., Eliceiri, K., Tomancak, P., Cardona, A., 2012. Fiji: an open-source platform for biological-image analysis. Nat. Methods 9, 676–682. https://doi.org/10.1038/nmeth.2019.

Shi, Y., Kirwan, P., Livesey, F.J., 2012. Directed differentiation of human pluripotent stem cells to cerebral cortex neurons and neural networks. Nat Protoc 7, 1836–1846. https://doi.org/10.1038/nprot.2012.116.

Sirugo, G., Williams, S.M., Tishkoff, S.A., 2019. The Missing Diversity in Human Genetic Studies. Cell 177, 26–31. https://doi.org/10.1016/j.cell.2019.02.048.

Veale, C.G.L., Edkins, A.L., Winks, S., Njoroge, M., Chibale, K., 2023. Including African data in drug discovery and development. Nat Rev Drug Discov 22, 521–522. https://doi.org/10.1038/d41573-023-00088-8.

Wonkam, A., 2021. Sequence three million genomes across Africa. Nature 590, 209–211. https://doi.org/10.1038/d41586-021-00313-7.